PNAS RESEARCH ARTICLE | MEDICAL SCIENCES

Deletion of TECRL promotes skeletal muscle repair by up-regulating EGR2

Sha Geng[a,b,c,1], Song-Bai Liu[d,1], Wei He[a,b,c,1], Xiangbin Pan[e,1], Yi Sun[f,1], Ting Xue[a,b,c], Shiyuan Han[a,b,c], Jing Lou[a,b,c], Ying Chang[a,b,c], Jiqing Zheng[a,b,c], Xinghong Shi[a,b,c], Yangxin Li[c,2], and Yao-Hua Song[a,b,c,2]

Edited by Louis Kunkel, Boston Children's Hospital, Harvard Medical School, Boston, MA; received November 12, 2023; accepted April 10, 2024

Myogenic regeneration relies on the proliferation and differentiation of satellite cells. TECRL (trans-2,3-enoyl-CoA reductase like) is an endoplasmic reticulum protein only expressed in cardiac and skeletal muscle. However, its role in myogenesis remains unknown. We show that TECRL expression is increased in response to injury. Satellite cell-specific deletion of TECRL enhances muscle repair by increasing the expression of EGR2 through the activation of the ERK1/2 signaling pathway, which in turn promotes the expression of PAX7. We further show that TECRL deletion led to the upregulation of the histone acetyltransferase general control nonderepressible 5, which enhances the transcription of EGR2 through acetylation. Importantly, we showed that AAV9-mediated TECRL silencing improved muscle repair in mice. These findings shed light on myogenic regeneration and muscle repair.

muscle regeneration | satellite cell | ischemia

Significance

Our study uncovered a role of TECRL (trans-2,3-enoyl-CoA reductase like) in regulating regenerative myogenesis. We deciphered a mechanism that enables the proliferation and differentiation of satellite cells through the downregulation of TECRL during muscle regeneration. TECRL regulates satellite cell function by controlling the levels of PAX7 via the ERK1/2/EGR2 signaling pathway. These findings can be exploited therapeutically to augment muscle regeneration by increasing the regenerative potential of satellite cells.

Satellite cells are local stem cells that reside in the skeletal muscle, which are normally in a quiescent state. In response to muscle injury, satellite cells are activated, reenter the cell cycle, and differentiate into myoblasts, which either fuse with each other or preexisting myofibers to complete the myogenic regeneration process (1–7). To maintain the satellite cell pool, a small portion of the satellite cells undergo a process called self-renewal and return back to a quiescent state.

The biogenesis, specification, and self-renewal of satellite cells are regulated by transcription factor paired box-protein-7 (Pax7), which is expressed at high levels in quiescent satellite cells, whereas MyoD is undetectable (6, 8–11). In differentiating myoblasts, the expression of Pax7 and MyoD is opposite to that in satellite cells, and Pax7 is undetectable in terminally differentiated cells. Pax7-deficient mice displayed impaired muscle regeneration due to a significant reduction in the number of satellite cells and myotubes (11–19). However, the mechanisms that regulate the expression of Pax7 are not completely understood.

TECRL (trans-2,3-enoyl-CoA reductase like) is an endoplasmic reticulum protein predominantly expressed in the heart and skeletal muscle (20). Loss of function mutation is associated with life-threatening arrhythmias and a high risk of sudden cardiac death. However, the functional role of TECRL in skeletal muscle remains unknown.

Egr2 belongs to a family of Cys2-His2 Zinc-finger transcription factors that also include *Egr1*, *Egr3*, and *Egr4* (21). *Egr2* can be induced by injury-associated cellular stress such as ischemia (22) and inflammation (23). *Egr2* is an important regulator of cell proliferation (24, 25) and differentiation (26, 27). Ectopic expression of *Egr2* in murine 3T3-L1 and NIH3T3 cells promotes adipogenesis (28).

In this study, using a satellite cell-specific TECRL knockout approach, we demonstrate that deletion of TECRL promotes satellite cell proliferation and myogenic regeneration. Furthermore, loss of TECRL resulted in upregulation of EGR2, which in turn augmented the gene expression of Pax7.

Results

TECRL Expression in Skeletal Muscle Is Mainly Restricted to Satellite Cells. In agreement with previous report (20), RT-qPCR showed very low levels of TECRL in adult mouse skeletal muscle. However, the expression of TECRL in skeletal muscle is increased after ischemia–reperfusion (IR) injury (Fig. 1*A* and *SI Appendix*, Fig. S1*A*). We also examined the expression of TECRL in the gastrocnemius (G) muscle of mdx mice, a Duchenne muscular dystrophy mouse model, at 3 and 5 wk of age, representing preonset and onset of the disease, respectively (29). The RT-qPCR results demonstrated a significant increase in TECRL expression at 5 wk compared to 3 wk (Fig. 1*B*). Furthermore, the expression of TECRL is also up-regulated in $BaCl_2$-injured muscle (Fig. 1*C*). Since the proliferation and differentiation of satellite cells are responsible for muscle repair, we analyzed the levels

Author affiliations: [a]Cyrus Tang Hematology Center, Collaborative Innovation Center of Hematology, Soochow University, National Clinical Research Center for Hematologic Diseases, The First Affiliated Hospital of Soochow University, Suzhou 215123, People's Republic of China; [b]State Key Laboratory of Radiation Medicine and Protection, Soochow University, Suzhou 215123, People's Republic of China; [c]Department of Cardiovascular Surgery of the First Affiliated Hospital & Institute for Cardiovascular Science, Soochow University, Suzhou Jiangsu 215000, People's Republic of China; [d]Suzhou Key Laboratory of Medical Biotechnology, Suzhou Vocational Health College, Suzhou 215009, People's Republic of China; [e]Department of Structural Heart Disease, National Center for Cardiovascular Disease, China and Fuwai Hospital, Chinese Academy of Medical Sciences and Peking Union Medical College, Beijing 100037, People's Republic of China; and [f]Department of Cardiovascular Surgery, Fuwai Yunnan Cardiovascular Hospital, Kunming 650102, People's Republic of China

Author contributions: X.P., Y.S., Y.L., and Y.-H.S. designed research; S.G., S.-B.L., W.H., T.X., S.H., J.L., Y.C., J.Z., and X.S. performed research; S.G., S.-B.L., W.H., X.P., Y.S., T.X., S.H., J.L., Y.C., J.Z., X.S., Y.L., and Y.-H.S. analyzed data; and X.P., Y.S., Y.L., and Y.-H.S. wrote the paper.

The authors declare no competing interest.

This article is a PNAS Direct Submission.

[1]S.G., S.-B.L., W.H., X.P., and Y.S. contributed equally to this work.

[2]To whom correspondence may be addressed. Email: yangxin_li@yahoo.com or yhsong@suda.edu.cn.

This article contains supporting information online at https://www.pnas.org/lookup/suppl/doi:10.1073/pnas.2317495121/-/DCSupplemental.

Published May 16, 2024.

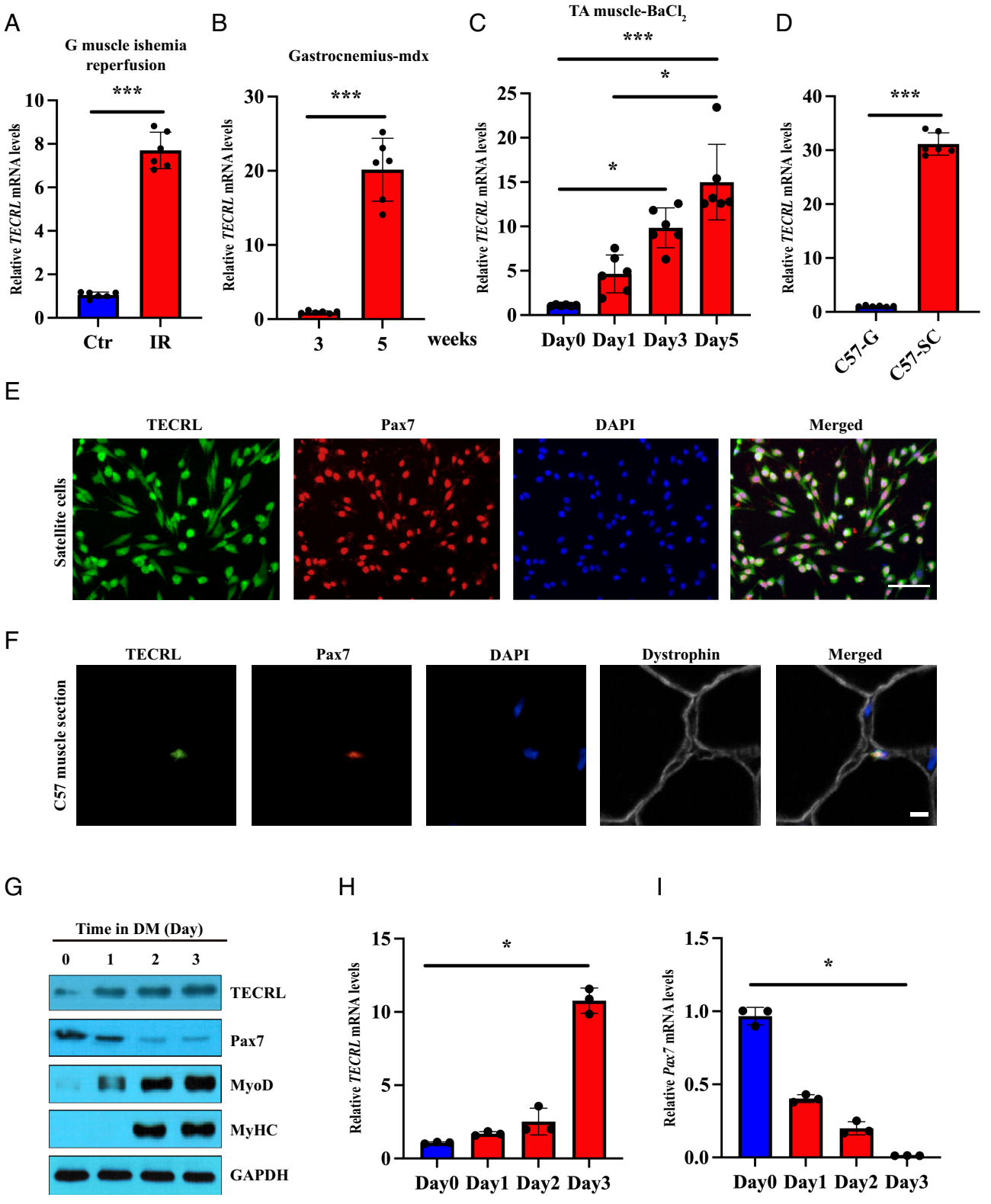

Fig. 1. TECRL expression in skeletal muscle is mainly restricted to satellite cells. (*A*) The mRNA level of *TECRL* was increased in IR injured gastrocnemius muscles (n = 6, values are mean ± SD, unpaired *t* test with Welch's correction, ***$P < 0.001$). (*B*) The mRNA levels of *TECRL* in the gastrocnemius muscles of 3 and 5-wk-old mdx mice (n = 6, values are mean ± SD, unpaired *t* test with Welch's correction, ***$P < 0.001$). (*C*) The mRNA levels of *TECRL* in $BaCl_2$-injured TA muscles (n = 6, values are mean ± SD, Kruskal–Wallis test with Dunn's multiple comparisons, ***$P < 0.001$, *$P < 0.05$). (*D*) RT-qPCR analysis of mRNA level of *TECRL* in gastrocnemius muscles and satellite cells (n = 6, values are mean ± SD, unpaired *t* test with Welch's correction, ***$P < 0.001$). (*E*) Immunostaining of TECRL (green) and Pax7 (red) in primary myogenic cells. Nuclei were labeled by DAPI (blue). (Scale bar: 50 μm.) (*F*) Cryosections from uninjured tibialis anterior muscles from wild-type C57BL/6J mice were stained for TECRL (green), Pax7 (red), and Dystrophin (gray). Nuclei were stained with DAPI (blue). The secondary antibodies used for detecting TECRL, Pax7, and Dystrophin were Alexa Fluor 568 goat anti-rabbit IgG (H+L), Alexa Fluor 488 goat anti-mouse IgG1 and Alexa Fluor 647 goat anti-mouse IgG2b, respectively. (Scale bar: 5 μm.) (*G*) Western blot analysis of the levels of TECRL, Pax7, MyoD, and MyHC in primary myogenic cells cultured in differentiation medium containing 2% horse serum. GAPDH was used as loading control. (*H* and *I*) The mRNA levels of *TECRL* and *Pax7* in primary myoblasts cultured in differentiation medium during a 3-d period (n = 3, values are mean ± SD, Kruskal–Wallis test with Dunn's multiple comparisons, *$P < 0.05$).

of TECRL in satellite cells. RT-qPCR showed much higher levels of TECRL in satellite cells compared to skeletal muscle (Fig. 1*D*). Immunostaining showed that satellite cells coexpress both TECRL and Pax7 (Fig. 1*E*). The colocalization of TECRL and Pax7 was verified by immunofluorescence staining of cryosections from the uninjured tibialis anterior muscle (TA muscle) of C57BL/6 mice using Pax7 and TECRL antibodies (Fig. 1*F*). TECRL expression can be found in both cytosol and nuclei (Fig. 1 *E* and *F*). The expression of MyoD, MyHC, and TECRL was increased while the levels of PAX7 were reduced in differentiating myoblasts (Fig. 1 *G–I*).

Deletion of TECRL in Satellite Cells Promotes Muscle Regeneration. To determine the role of TECRL in myogenesis, we generated satellite cell–specific TECRL knockout mice ($TECRL^{scko}$) by crossing $TECRL^{flox/flox}$ mice with Pax7-Cre mice (*SI Appendix*, Fig. S1*B*), and the genotype was confirmed by PCR (*SI Appendix*, Fig. S1*C*). The efficiency of TECRL deletion in satellite cells was verified by RT-qPCR (*SI Appendix*, Fig. S1*D*).

Deletion of TECRL in satellite cells resulted in a significant increase in body size, body and muscle weight, and grip strength compared with littermate $TECRL^{flox/flox}$ mice (*SI Appendix*, Fig. S2 *A–F*). The total number of muscle satellite cells (SCs) of $TECRL^{flox/flox}$ and $TECRL^{scko}$ mice were analyzed via flow cytometry and then normalized to muscle weight (per gram) (*SI Appendix*, Fig. S1*E*). Compared to $TECRL^{flox/flox}$ mice, $TECRL^{scko}$ mice exhibited a significant increase in the number of SCs (*SI Appendix*, Fig. S2*G*). H&E staining revealed a significant increase in both the number and size of muscle fibers in $TECRL^{scko}$ mice compared to $TECRL^{flox/flox}$ mice (*SI Appendix*, Fig. S2 *H–J*). $BaCl_2$ solution was locally injected into the TA muscles of adult $TECRL^{flox/flox}$ and $TECRL^{scko}$ mice to assess how TECRL deletion might impact muscle regeneration. After the injury, muscle weight reduction was less severe in the $TECRL^{scko}$ mice compared with the $TECRL^{flox/flox}$ mice (Fig. 2 *A* and *B*). H&E staining showed that the number of newly formed centronucleated myofibers (CNF) and cross-sectional area (CSA) of CNF was higher in the TA muscle of $TECRL^{scko}$ mice than that of littermate $TECRL^{flox/flox}$ mice (Fig. 2 *C–F*). The reconstitution of muscle structure was completed on day 10 after injury in $TECRL^{scko}$ mice, whereas muscle sections of the $TECRL^{flox/flox}$ mice still showed areas of fibrosis (Fig. 2*C*). Muscle necrosis was also less severe in the $TECRL^{scko}$ TA muscle than that of $TECRL^{flox/flox}$ on day 5 after injury (Fig. 2*G*).

The appearance of the embryonic isoform of MyHC (eMyHC) is an indicator of muscle regeneration (30). The increased number and CSA of $eMyHC^+$ fibers in injured muscles from $TECRL^{scko}$ mice can be seen as early as day 3 after injury when compared with $TECRL^{flox/flox}$ mice (Fig. 3 *A–C*). The mRNA level of eMyHC (*Myh3*) in $TECRL^{scko}$ muscles was higher than that of $TECRL^{flox/flox}$ muscles (Fig. 3*D*). The expression of eMyHC protein can be detected as early as day 3 after injury in $TECRL^{scko}$ muscles, whereas it was not detected until day 5 in the $TECRL^{flox/flox}$ muscles (Fig. 3*E*).

These findings were confirmed using an IR injury model of the mouse hindlimb. Compared to the control, $TECRL^{scko}$ muscle displayed better regeneration (*SI Appendix*, Fig. S3*A*), reduced fibrosis (*SI Appendix*, Fig. S3*B*), increased number of satellite cells (*SI Appendix*, Fig. S3 *C* and *D*), and upregulation of Pax7 expression (*SI Appendix*, Fig. S3 *E* and *F*). This observation could potentially contribute to the accelerated regeneration observed in the absence of TECRL.

Compared to the control, the $TECRL^{scko}$ muscle displayed an increased number of $eMyHC^+$ fibers up to 14 d postinjury, which was then decreased after 28 d when muscle regeneration was near completion (*SI Appendix*, Fig. S4*A*). The increased expression of eMyHC mRNA (*Myh3*) in $TECRL^{scko}$ muscles was confirmed by RT-qPCR (*SI Appendix*, Fig. S4*B*). Western blot showed that the expression of eMyHC protein appeared 7 d after injury in $TECRL^{scko}$ muscles vs. 14 d in $TECRL^{flox/flox}$ muscles (*SI Appendix*, Fig. S4*C*). These data suggest that muscle regeneration was enhanced by deleting TECRL in satellite cells.

The formation of new myofibers requires the activation and differentiation of $Pax7^+$ satellite cells. Immunofluorescence staining of muscle sections revealed an increased number of $Pax7^+$ cells in $TECRL^{scko}$ mice vs. $TECRL^{flox/flox}$ mice upon injury induced by $BaCl_2$ (Fig. 4 *A* and *B*). The increased expression of Pax7 was verified by RT-qPCR and western blot (Fig. 4 *C* and *D*). Consistent with the above data, $TECRL^{-/-}$ myoblasts exhibited increased Pax7 expression compared with $TECRL^{+/+}$ myoblasts (Fig. 4 *E–H*). Loss of TECRL also enhanced the proliferation of primary myoblasts as evidenced by more $Pax7^+Ki67^+$ cells in $TECRL^{-/-}$ cultures (Fig. 5 *A* and *B*), and an increased number of cells during a 5-d period (Fig. 5*C*). Colony forming assay showed that $TECRL^{-/-}$ myogenic cells formed more and larger colonies compared to $TECRL^{+/+}$ cells (Fig. 5 *D–F*), suggesting that deletion of TECRL may play a role in regulating satellite cell quiescence and activation. We then isolated single myofibers from the extensor digitorum longus (EDL) muscle of $TECRL^{flox/flox}$ and $TECRL^{scko}$ mice, and satellite cells were identified by immunostaining of Pax7 or MyoD. $Pax7^+/MyoD^-$ and $Pax7^+MyoD^+$ are considered as quiescent and activated satellite cells, respectively (31). Compared to the control, freshly isolated $TECRL^{scko}$ myofibers displayed an increased number of quiescent satellite cells ($Pax7^+/MyoD^-$) (Fig. 5 *G–I*). After 72 h in culture, these satellite cells formed clusters, and the clusters of $TECRL^{scko}$ myofibers contained more activated satellite cells ($Pax7^+MyoD^+$) compared to the control (Fig. 5 *G*, *J*, and *K*). These results suggest that loss of TECRL enhances the proliferation of activated myoblasts.

Myogenic differentiation requires the expression of MyoD and myogenin, which were increased in the TA muscle of $TECRL^{scko}$ mice vs. $TECRL^{flox/flox}$ mice after the injury, as shown by western blot (*SI Appendix*, Fig. S5 *A–C*) and immunofluorescence analysis (*SI Appendix*, Fig. S5 *D–G*). $TECRL^{scko}$ muscles also exhibited increased EdU^+ cells 5 d after injury (*SI Appendix*, Fig. S5 *D* and *G*). These findings indicate that muscle regeneration was enhanced by deleting TECRL. Collectively, these findings indicate that loss of TECRL enhances satellite cell activation, proliferation, and differentiation.

To confirm these findings, we examined MyHC expression by western blot. The results showed that TECRL deletion enhances MyHC expression during myoblast differentiation (*SI Appendix*, Fig. S6*A*). Western blot results also demonstrated elevated levels of MyoD in $TECRL^{-/-}$ myoblasts compared to $TECRL^{+/+}$ cells on the third-day postdifferentiation (*SI Appendix*, Fig. S6*B*). In line with these results, immunofluorescence staining revealed that TECRL deletion promotes the formation of myotubes, with a higher differentiation index and fusion index in the $TECRL^{-/-}$ group (*SI Appendix*, Fig. S6 *C–E*). Furthermore, the number of $Pax7^+$ cells associated with myotubes was greater in $TECRL^{-/-}$ cells than in $TECRL^{+/+}$ cells (*SI Appendix*, Fig. S6 *C* and *F*), indicating increased satellite cell progeny production in the absence of TECRL.

TECRL Deletion–Induced Satellite Cell Activation and Proliferation Is Mediated by EGR2. To decipher the signaling pathways downstream of TECRL, we performed RNA sequencing (RNAseq) on gastrocnemius muscles from $TECRL^{scko}$ mice and $TECRL^{flox/flox}$ mice. Compared to the $TECRL^{flox/flox}$ muscle, the

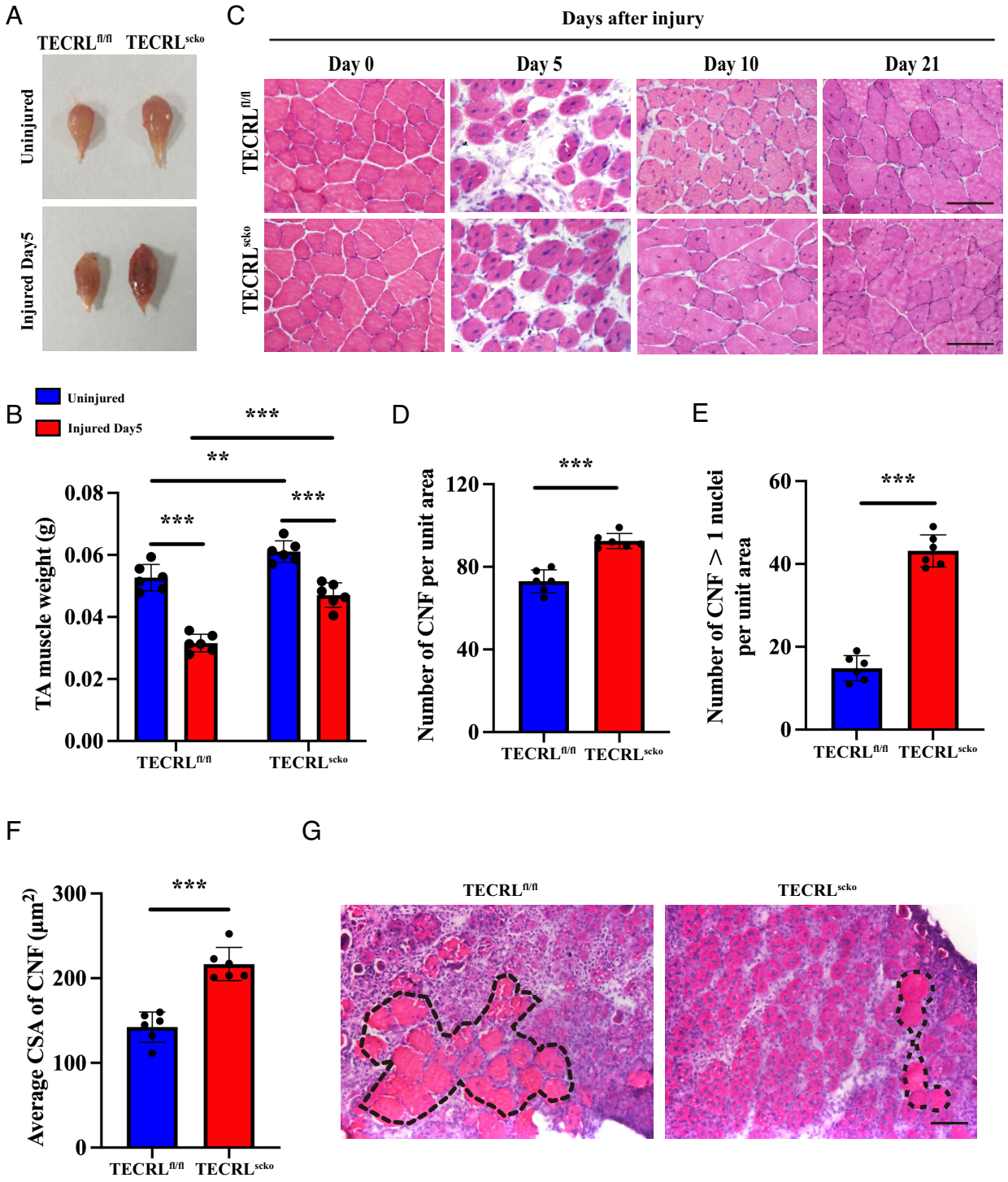

Fig. 2. Loss of TECRL enhances skeletal muscle regeneration. (*A*) Representative images of injured and uninjured tibialis anterior muscles from TECRL$^{flox/flox}$ and TECRL^{scko} mice. (*B*) Average wet weight of TA muscles (n = 6, values are mean ± SD, ANOVA with post hoc Tukey's multiple comparisons, ***P < 0.001, **P < 0.01). (*C*) H&E staining of TA muscles from TECRL^{scko} and TECRL$^{flox/fox}$ littermates after $BaCl_2$ injection and uninjured muscles. (Scale bar: 50 µm.) (*D*) Number of centronucleated fibers (CNF) per field (0.04 mm^2) on day 5 post injury (n = 6, values are mean ± SD, unpaired t test, ***P < 0.001). (*E*) The number of muscle fibers containing more than one central nucleus per field (0.04 mm^2) (n = 6, values are mean ± SD, unpaired t test, ***P < 0.001). (*F*) The average CSA of CNF of regenerated muscle fibers (n = 6, values are mean ± SD, unpaired t test, ***P < 0.001). (*G*) H&E staining of TA muscles from TECRL^{scko} and TECRL$^{flox/flox}$ at day 5 after $BaCl_2$ injection. The black-dotted line shows necrosis. (Scale bar: 50 µm.)

TECRL^{scko} muscle displayed a set of differentially regulated genes that are greater than twofold (306 up and 135 down) (*SI Appendix*, Fig. S7*A*). Gene Ontology (GO) analysis of our RNA-seq data revealed 15 up-regulated genes involved in the muscle tissue development pathway. Among them, EGR2 emerged as the top-ranking transcription factor binding to the Pax7 promoter (*SI Appendix*, Fig. S7*B*), exhibiting a 5.97-fold increase in the TECRL^{scko} muscle. This observation was confirmed by RT-qPCR (*SI Appendix*, Fig. S7 *C* and *D*). However, RNAseq on gastrocnemius muscles from TECRL^{scko} mice and TECRL$^{flox/flox}$ mice showed no difference in the expression of EGR1. The results were confirmed by RT-qPCR (*SI Appendix*, Fig. S8*A*).

To explore the potential link between TECRL, EGR2, and Pax7, we performed gain and loss of function studies. TECRL

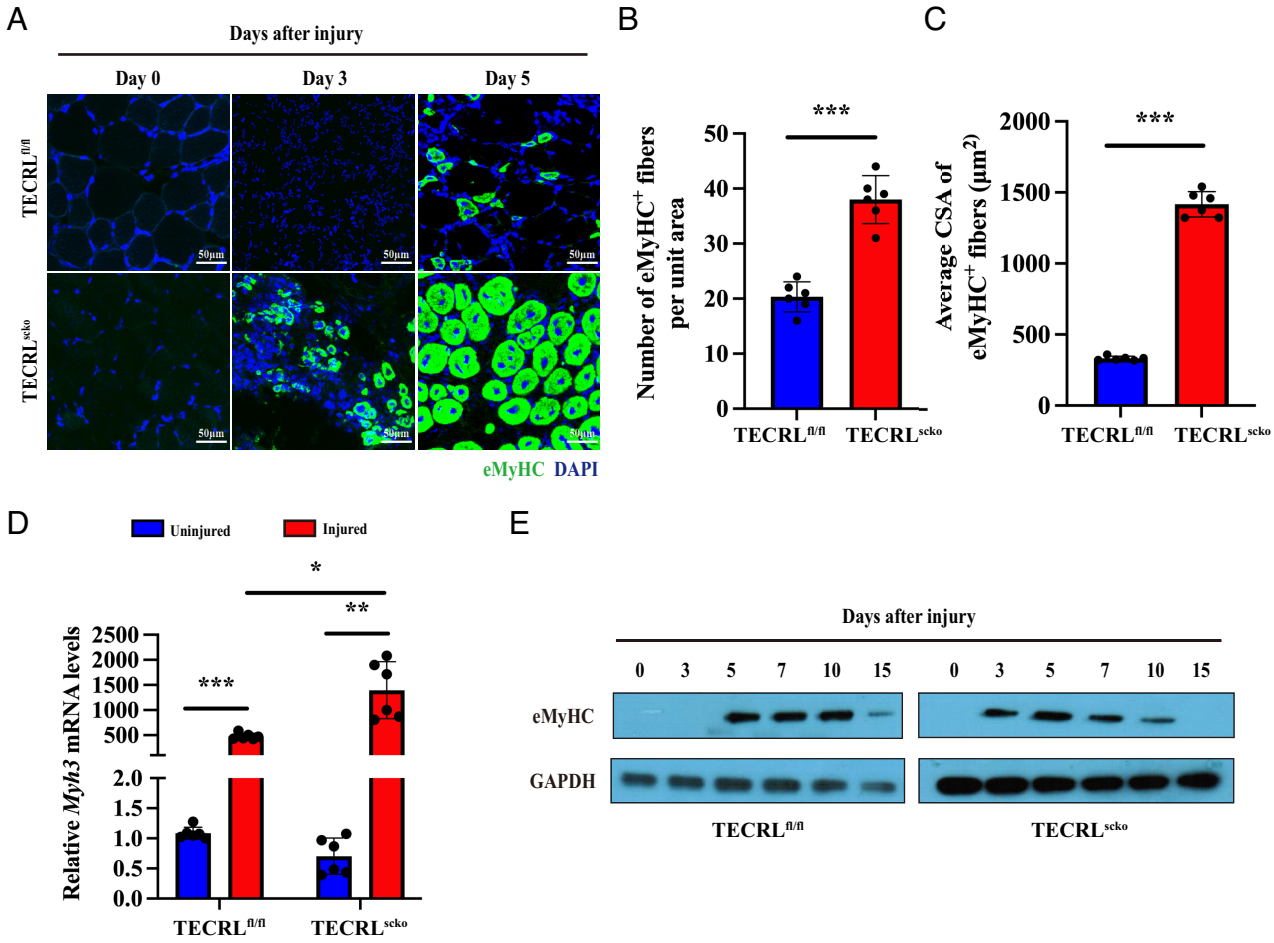

Fig. 3. Deletion of TECRL in satellite cells increased expression of eMyHC. (*A*) Immunostaining of eMyHC (green) for regenerating myofibers in TA muscles from TECRL$^{flox/flox}$ and TECRL^{scko} mice at different time points after $BaCl_2$-induced injury and uninjured muscles. The nuclei were stained with DAPI (blue). (Scale bar: 50 μm.) (*B* and *C*) Quantification of the numbers (n = 6, values are mean ± SD, unpaired *t* test, ***$P < 0.001$) and CSA of eMyHC$^+$ fibers per field in TA muscles 5 d after injury (n = 6, values are mean ± SD, unpaired *t* test with Welch's correction, ***$P < 0.001$). (*D*) RT-qPCR analysis of relative mRNA levels of *Myh3* (eMyHC mRNA) in TA muscles 3 d after injury (n = 6, values are mean ± SD, Brown–Forsythe and Welch ANOVA tests with post hoc Dunnett's T3 multiple comparisons, ***$P < 0.001$, **$P < 0.01$, *$P < 0.05$). (*E*) Western blot analysis of eMyHC in TA muscles of TECRL$^{flox/flox}$ and TECRL^{scko} mice at different time points after $BaCl_2$ injection.

deletion in primary myoblasts resulted in an increased level of EGR2 and Pax7 compared with the control cells (*SI Appendix*, Fig. S7 *E* and *F*). Overexpression EGR2 in primary myoblasts led to an increased *Pax7* mRNA level as compared to the control (*SI Appendix*, Fig. S7 *G* and *H*), suggesting that Pax7 expression is regulated by EGR2. Along this line, the proliferation of myoblasts was inhibited by EGR2 knockdown (Fig. 6*A*). Compared to *TECRL*$^{+/+}$ cells, *Pax7* mRNA level was increased in *TECRL*$^{-/-}$ cells, and this effect was abolished by silencing EGR2 (Fig. 6*B*). Pax7 expression was enhanced by overexpressing EGR2 (Fig. 6*C*). It has been shown that the expression of EGR2 can be up-regulated by activating the ERK1/2 signaling pathway (32). GO analysis revealed an upregulation of ERK1 and ERK2 cascade, positioned at the top of up-regulated genes associated with muscle tissue development, positive regulation of cell cycle, stem cell differentiation, and striated muscle cell proliferation (*SI Appendix*, Fig. S7*B*). This led us to explore the potential involvement of ERK1/2 in the TECRL/EGR2 pathway. Compared to *TECRL*$^{+/+}$ cells, *TECRL*$^{-/-}$ cells exhibited an increased level of phospho–ERK1/2 (Fig. 6 *D* and *E*), suggesting that loss of TECRL led to activation of the ERK1/2 pathway. Consistent with these findings, the expression of EGR2 and Pax7 was reduced when myoblasts were treated with ERK1/2 inhibitor PD184352 (Fig. 6 *F* and *G*). Similarly, PD184352 treatment of myofibers resulted in a reduced number of clusters and the number of Pax7$^+$MyoD$^+$ cells per cluster (Fig. 6 *H*–*J*). These results indicate that TECRL deletion triggers the activation of the ERK1/2 signaling pathway, subsequently activating EGR2 to induce the expression of Pax7 and the proliferation of satellite cells.

In line with these findings, the ChIP assay showed an enrichment of EGR2 in Pax7 promoter at 2 consensus sites (Fig. 6*K*), and these enrichments were significantly increased in *TECRL*$^{-/-}$ myoblast compared with the control cells (Fig. 6*L*). To determine whether Pax7 promoter can be activated by EGR2, we performed a dual-luciferase reporter assay. Primary myoblasts were transfected with a plasmid expressing Pax7 promoter-driven luciferase and a plasmid expressing EGR2. The assay revealed an increased luciferase activity in myoblasts transfected with EGR2 plasmid compared with the control (Fig. 6*M*). It has been shown that EGR2 transcription can be activated by GCN5 (general control nonderepressible 5)-mediated acetylation (33). Previous studies also highlighted the role of GCN5-mediated acetylation in positively regulating EGR2 transcriptional activity, crucial for the development of CD1d-restricted invariant natural killer T cells (33). Furthermore, GCN5 has been shown to maintain muscle integrity and promote dystrophin expression by acetylating YY1 (34). Importantly, GO analysis showed that genes involved in acetylation-dependent protein binding were significantly up-regulated (*SI Appendix*, Fig. S7*B*), suggesting that the increase of EGR2 in the TECRL^{scko} muscle may be associated with protein acetylation. Consequently, we focused on the GCN5/EGR2

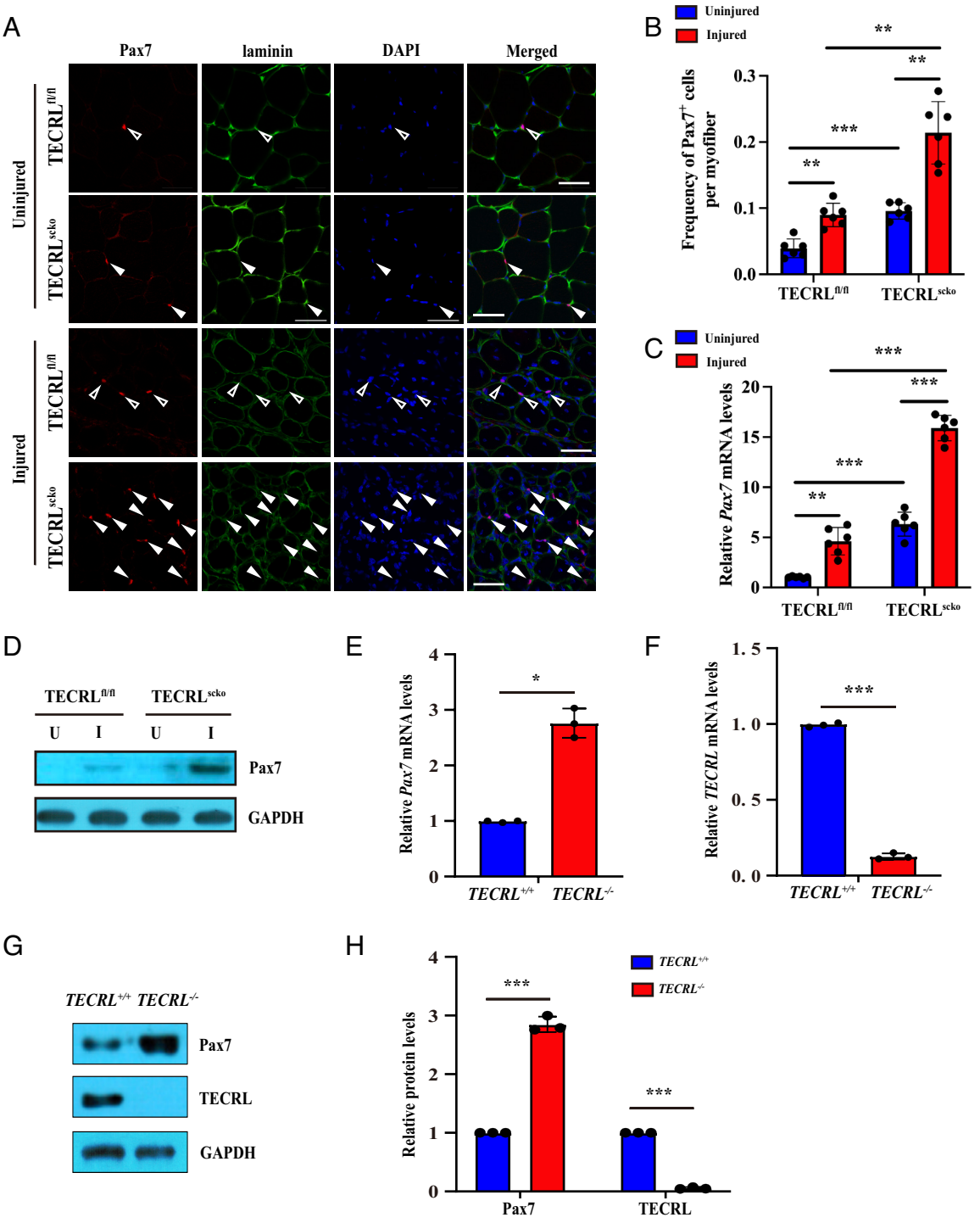

Fig. 4. Deletion of TECRL enhances the expression of Pax7. (*A*) Immunostaining with Pax7 (red) and laminin (green) showing an increased number of satellite cells (white arrows) in uninjured and $BaCl_2$-injured TA muscles of $TECRL^{scko}$ mice compared to $TECRL^{flox/flox}$ mice. (Scale bar: 50 μm.) (*B*) Quantification of the average number of $Pax7^+$ cells per myofiber in TA muscles of $TECRL^{flox/flox}$ and $TECRL^{scko}$ mice (n = 6, values are mean ± SD, Brown–Forsythe and Welch ANOVA tests with post hoc Dunnett's T3 multiple comparisons, $^{***}P < 0.001$, $^{**}P < 0.01$). (*C*) RT-qPCR analysis of relative mRNA levels of *Pax7* in uninjured and injured TA muscles (n = 6, values are mean ± SD, Brown–Forsythe and Welch ANOVA tests with post hoc Dunnett's T3 multiple comparisons, $^{***}P < 0.001$, $^{**}P < 0.01$). (*D*) Western blot analysis of Pax7 in TA muscles. U: uninjured, I: injured. (*E* and *F*) RT-qPCR analysis of mRNA levels of *Pax7* and *TECRL* in $TECRL^{+/+}$ and $TECRL^{-/-}$ primary myogenic cells (n = 3, values are mean ± SD, unpaired *t* test, $^{***}P < 0.001$, $^{*}P < 0.05$). (*G*) Western blot analysis of protein levels of Pax7 and TECRL in $TECRL^{+/+}$ and $TECRL^{-/-}$ primary myogenic cells. (*H*) Densitometric quantification of relative protein levels of Pax7 and TECRL (n = 3, values are mean ± SD, unpaired *t* test, $^{***}P < 0.001$).

pathway to determine whether TECRL deletion led to the upregulation of GCN5, which, in turn, enhances the expression of EGR2 through acetylation, leading to increased expression of Pax7.

RT-qPCR results showed the mRNA level of *GCN5* was significantly up-regulated in $TECRL^{-/-}$ cells (Fig. 6*N*). Western blot showed that the levels of GCN5, Pax7, and acetylated EGR2 (Ac-EGR2) were increased in $TECRL^{-/-}$ cells compared to $TECRL^{+/+}$ cells (Fig. 6*O*). However, the increased expression of Pax7 and Ac-EGR2 was reduced in the presence of a specific GCN5 inhibitor CPTH2 (Fig. 6*O*). These results suggest that deletion of TECRL resulted in an increased expression of GCN5, which in turn enhances EGR2 transcription. To determine whether GCN5 alters

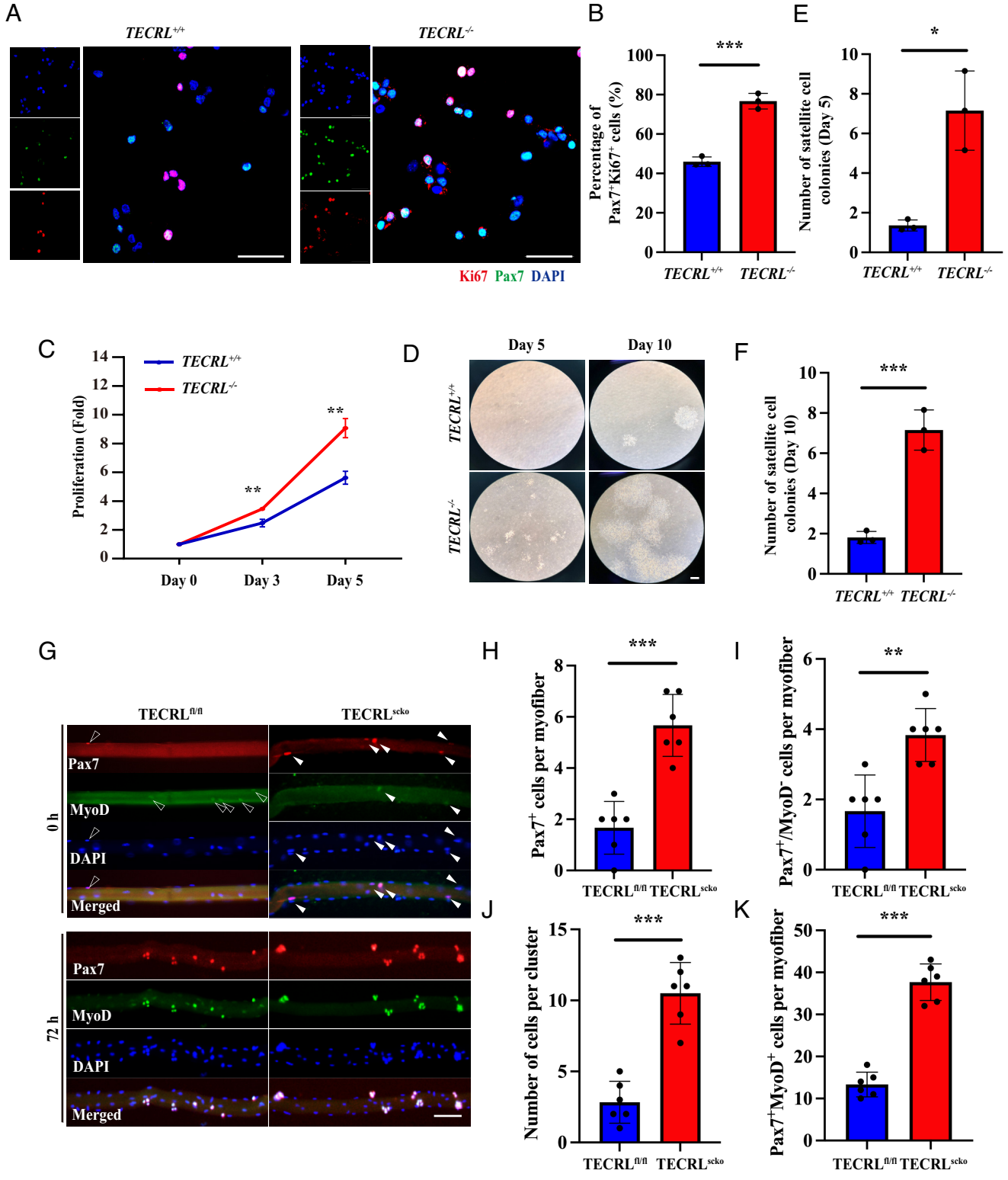

Fig. 5. TECRL regulates satellite cell proliferation. (*A*) Immunostaining of Pax7 (green) and Ki67 (red) in *TECRL*$^{+/+}$ and *TECRL*$^{-/-}$ primary myoblasts cultured for 3 d. The cells were incubated with anti-Ki67 (1:50 dilution) at 4 °C overnight. (Scale bar: 50 μm.) (*B*) The percentage of Pax7^{+}Ki67^{+} cells from *TECRL*$^{+/+}$ and *TECRL*$^{-/-}$ myoblasts (n = 3, values are mean ± SD, unpaired *t* test, ***P < 0.01). (*C*) Cell proliferation was performed by plating *TECRL*$^{+/+}$ and *TECRL*$^{-/-}$ primary myoblasts at the same density and culturing for 5 d (n = 3, values are mean ± SD, unpaired *t* test, **P < 0.01). The cells were enumerated at different time points. (*D*) Colony forming assay for freshly isolated *TECRL*$^{+/+}$ and *TECRL*$^{-/-}$ primary myogenic cells. (Scale bar: 100 μm.) (*E*) Quantification of the number of satellite cell colonies after 5 d in culture (n = 3, values are mean ± SD, unpaired *t* test with Welch's correction, *P < 0.05). (*F*) Quantification of the number of satellite cell colonies after 10 d in culture (n = 3, values are mean ± SD, unpaired *t* test, ***P < 0.001). (*G*) Single myofibers were isolated from the EDL muscle of TECRL$^{flox/flox}$ and TECRL^{scko} mice. The myofibers collected either immediately after isolation or after 72 h of culture were immunostained for Pax7 (red) or MyoD (green). Nuclei were identified by staining with DAPI (blue). (Scale bar: 100 μm.) (*H*) Quantification of the number of Pax7^{+} cells in each myofibers immediately after isolation (n = 6, values are mean ± SD, unpaired *t* test, ***P < 0.001). (*I*) Quantification of the number of Pax7^{+}/MyoD^{-} cells in each myofibers immediately after isolation (n = 6, values are mean ± SD, unpaired *t* test, **P < 0.01). (*J*) Quantification of the number of cells in each cluster on cultured myofibers (n = 6, values are mean ± SD, unpaired *t* test, ***P < 0.001). (*K*) Quantification of the number of Pax7^{+}MyoD^{+} cells on cultured myofibers (n = 6, values are mean ± SD, unpaired *t* test, ***P < 0.001). Analysis was performed on 6 to 10 myofibers for each mouse at each time point.

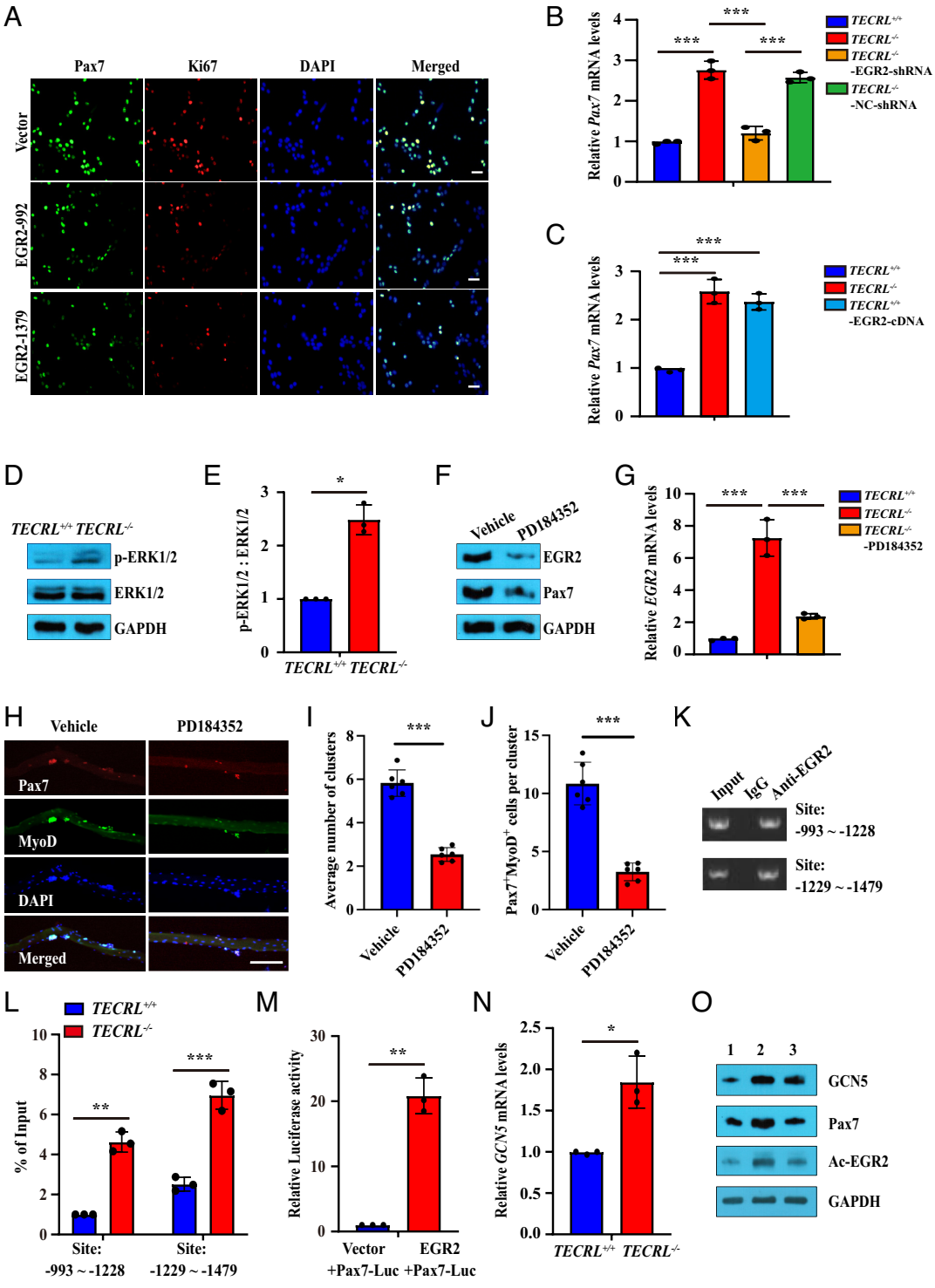

Fig. 6. TECRL deletion led to activation of the ERK1/2 signaling pathway, which then activates EGR2 to induce the expression of Pax7 and the proliferation of satellite cells. (*A*) Immunostaining of Pax7 (green) and Ki67 (red) in primary myoblasts transduced with the empty vector or shRNA-EGR2 lentiviral construct cultured for 3 d. (Scale bar: 50 μm.) (*B*) The mRNA level of *Pax7* in $TECRL^{+/+}$, $TECRL^{-/-}$, $TECRL^{-/-}$-EGR2-shRNA, and $TECRL^{-/-}$-NC-shRNA in primary myoblasts (n = 3, values are mean ± SD, one-way ANOVA tests with post hoc Tukey's multiple comparisons, $^{***}P < 0.001$). (*C*) The mRNA level of *Pax7* in $TECRL^{+/+}$, $TECRL^{-/-}$, and $TECRL^{+/+}$-EGR2-cDNA in primary myoblasts (n = 3, values are mean ± SD, one-way ANOVA tests with post hoc Tukey's multiple comparisons, $^{***}P < 0.001$). (*D*) Western blot analysis of phosphorylated and total ERK1/2 in $TECRL^{+/+}$ and $TECRL^{-/-}$ cultures. (*E*) Ratio of phospho-ERK1/2 and total ERK1/2 in $TECRL^{+/+}$ and $TECRL^{-/-}$ primary myoblasts (n = 3, values are mean ± SD, unpaired *t* test with Welch's correction, $^{*}P < 0.05$). (*F*) Western blot analysis of Pax7 and EGR2 in primary myoblasts in the presence of ERK1/2 inhibitors (PD184352) or vehicle. (*G*) The mRNA level of *EGR2* in $TECRL^{+/+}$, $TECRL^{-/-}$, and $TECRL^{-/-}$ primary myoblasts in the presence of PD184352 (n = 3, values are mean ± SD, one-way ANOVA tests with post hoc Tukey's multiple comparisons, $^{***}P < 0.001$). (*H*) Single myofibers isolated from EDL muscle of WT mice were cultured in satellite cell growth medium in the presence of ERK1/2 inhibitors (PD184352) or vehicle for 72 h. The single myofibers were stained for Pax7 (red) and MyoD (green). Nuclei were identified by staining with DAPI (blue). (Scale bars: 100 μm.) (*I*) Quantification of the number of cell clusters on each myofiber (n = 6, values are mean ± SD, unpaired *t* test, $^{***}P < 0.001$). (*J*) Quantification of the number of $Pax7^{+}MyoD^{+}$ cells per cluster (n = 6, values are mean ± SD, unpaired *t* test, $^{***}P < 0.001$). Analysis was performed using 3-6 myofibers for each mouse in each group. (*K*) Primary myoblasts were processed for ChIP assay. The semiquantitative RT-qPCR showing EGR2 was enriched at the indicated sites of the Pax7 promoter. The numbers represent the location of the consensus sequence upstream of the first ATG of the Pax7 gene. (*L*) RT-qPCR analysis of ChIP product to determine the percentage of EGR2 input enrichment at specific sites in the Pax7 promoter in $TECRL^{+/+}$ and $TECRL^{-/-}$ cultures (n = 3, values are mean ± SD, unpaired *t* test, $^{***}P < 0.001$, $^{**}P < 0.01$). (*M*) Dual-luciferase reporter assay of Pax7 promoter activation by EGR2. WT myoblasts were cotransfected with 250 ng empty Vector or EGR2-cDNA, 250 ng Pax7-Luc, and 20 ng pRL-TK plasmid by Lipofectamine 2000 (n = 3, values are mean ± SD, unpaired *t* test with Welch's correction, $^{**}P < 0.01$). (*N*) RT-qPCR analysis of *GCN5* in $TECRL^{+/+}$ and $TECRL^{-/-}$ cultures (n = 3, values are mean ± SD, unpaired *t* test, $^{*}P < 0.05$). (*O*) Western blot analysis of GCN5, Pax7, and Ac-EGR2 levels in $TECRL^{+/+}$, $TECRL^{-/-}$, and $TECRL^{-/-}$-CPTH2 cultures. EGR2 proteins in the lysates of $TECRL^{+/+}$, $TECRL^{-/-}$, and $TECRL^{-/-}$-CPTH2 cultures were immunoprecipitated with the EGR2 antibodies, followed by immunoblotting with an anti-acetyl lysine–specific antibody to detect acetylated proteins. 1: $TECRL^{+/+}$, 2: $TECRL^{-/-}$, 3: $TECRL^{-/-}$-CPTH2. CPTH2 (0.05M) was added to the cell culture medium for 12 h.

the expression of EGR1, we performed a western blot analysis of GCN5 and EGR1 levels using $TECRL^{+/+}$ and $TECRL^{-/-}$ myoblasts. The results showed that compared to $TECRL^{+/+}$ cells, the expression of GCN5 is increased in $TECRL^{-/-}$ cells, but there was no significant change in the expression of EGR1 (*SI Appendix*, Fig. S8*B*).

GO analysis revealed a significant upregulation of genes regulating the transition between fast and slow muscle fibers (*SI Appendix*, Fig. S7*B*). Given the role of TERCL in mitochondria and metabolic function, we performed immunofluorescence staining on muscle sections of uninjured $TECRL^{scko}$ and $TECRL^{flox/flox}$ mice using

primary antibodies against type I, IIa, and IIb (type IIx expression was inferred from unstained fibers). The fiber typing results revealed a significant increase in the proportion of glycolytic muscle fibers (IIb and IIx) and a decrease in the proportion of oxidized muscle fibers (I/IIa) in the gastrocnemius muscles of TECRL^{scko} mice compared to TECRL$^{flox/flox}$ mice (*SI Appendix*, Fig. S8 *C* and *D*). GO analysis also revealed an upregulation of genes regulating the positive regulation of the cell cycle (*SI Appendix*, Fig. S7*B*). To determine whether deletion of TECRL influences cell cycle kinetics, we analyzed the cell cycle of primary myoblasts from TECRL$^{flox/flox}$ and TECRL^{scko} mice by flow cytometry. Under normal growth conditions, the myoblast population in the S+G_2/M phase was significantly larger in myoblasts from TECRL^{scko} mice compared to those from TECRL$^{flox/flox}$ mice (*SI Appendix*, Fig. S8 *E–G*), indicating that the deletion of TECRL promotes cell proliferation.

AAV9-Mediated TECRL Silencing Improved Muscle Repair. To develop a potential therapy for IR injury, we engineered a recombinant AAV9 vector containing shRNA targeting TECRL [shRNA (*Tecrl*)-AAV], which was injected into the gastrocnemius muscle of IR-injured mice. The knockdown of TECRL in the gastrocnemius muscles and satellite cells of the shRNA (*Tecrl*)-AAV-treated mice was verified by RT-qPCR (*SI Appendix*, Fig. S9*A*). Green fluorescent protein signals were readily detectable in the injected muscles, further confirming that the adenovirus transduction was successful (*SI Appendix*, Fig. S9*B*). H&E and CD45 staining showed enhanced muscle regeneration (*SI Appendix*, Fig. S9 *C–E*) and reduced inflammatory cell infiltration (*SI Appendix*, Fig. S9 *F* and *G*) in shRNA (*Tecrl*)-AAV treated mice compared with the control. Moreover, the number of myogenin$^+$ cells (*SI Appendix*, Fig. S9 *H* and *I*) and the number of eMyHC$^+$ myofibers (*SI Appendix*, Fig. S9 *J–L*) were increased in gastrocnemius muscle of shRNA (*Tecrl*)-AAV treated mice vs. control. These results indicate that AAV9-mediated TECRL silencing improved muscle repair.

Discussion

In the present study, we demonstrate that deletion of TECRL in satellite cells enhanced their proliferation and differentiation through upregulation of EGR2 and Pax7, leading to improved myogenic regeneration after injury.

EGR2 plays an important role in both development and response to tissue injury. EGR2 mutations cause a significant reduction of anterior digastric and mylohyoid muscles (35). EGR2 controls cell fate by repressing neutrophil genes during macrophage differentiation (26). Overexpression of EGR2 protects the rat brain from ischemic injury (36). These previous studies are in line with our data that the proliferation of myoblasts was inhibited by EGR2 knockdown.

We further showed that EGR2 expression is regulated by GCN5 through acetylation, which agrees with previous reports that GCN5-mediated acetylation of PGC-1α is responsible for the switch from glucose to fatty acid oxidation during nutrient deprivation in skeletal muscle (37). GCN5 was found to maintain muscle integrity by acetylating YY1 to promote dystrophin expression (34). GCN5-deleted embryoid bodies display deficient activation of ERK and mislocalization of cytoskeletal components (38).

We demonstrated that TECRL deletion-induced Pax7 upregulation is mediated through the ERK1/2/EGR2 signaling pathway. ChIP assay showed high enrichment of EGR2 in *Pax7* promoter at two consensus sites in satellite cells from WT mice. RT-qPCR revealed that the fold enrichment of EGR2 to specific binding sites in the *Pax7* promoter was significantly increased in the absence of TECRL. These findings are consistent with the previous reports that EGR2 is activated by ERK1/2 in L6 myotubes (39) and in osteroblasts (40). β1-integrin and FGF2-induced satellite cell self-renew and expansion are mediated by ERK1/2, and augmenting β1-integrin activity with a monoclonal antibody enhances the regeneration and function of dystrophic muscles in mdx mice (41). Akirin2 enhances the proliferation and differentiation of satellite cells by activating the ERK1/2 pathway (42). Loss of CRY2 activates the ERK1/2 signaling pathway and ETS1, which binds to the promoter of Pax7 to induce its transcription (43). Inactivation of ERK1/2 in MM14 myoblasts prevents myoblast proliferation (44). TA muscles from mdx mice showed reduced endogenous activation of ERK1/2 compared with normal TA muscles (45). These findings are in line with our results that the ERK1/2/EGR2 signaling pathway plays an essential role in satellite cell proliferation and muscle repair.

Our findings indicate a significant increase in both the number and size of muscle fibers in TECRL^{scko} mice at baseline compared to TECRL$^{flox/flox}$ mice. This might explain why TECRL deletion in satellite cells affects the number of intact muscle fibers 5 d post $BaCl_2$ injection.

IR injury is known to cause skeletal muscle mitochondrial dysfunction in both humans and animals (46). Recent evidence underscores the pivotal role of mitochondria as central regulators of inflammation, orchestrating fundamental cellular responses to stressors (47). Damaged or dysfunctional mitochondria release signals known as mitochondrial-derived damage-associated molecular patterns (mito-DAMPs) that are recognized by the innate immune system and modulate postinjury inflammatory cell recruitment (48, 49). Our data show that deletion of TECRL resulted in a significant increase in the proportion of glycolytic muscle fibers (IIb and IIx) and a decrease in the proportion of oxidized muscle fibers (I/IIa) in the gastrocnemius muscles of TECRL ^{scko} mice compared to TECRL$^{flox/flox}$ mice. It is known that glycolytic muscle fibers contain fewer mitochondria than oxidative fibers (50). Consequently, the reduced quantity of mito-DAMPs released upon IR injury in the absence of TECRL may account for the observed decrease in the number of infiltrating CD45$^+$ cells.

In summary, our study uncovered a role of TECRL in regulating regenerative myogenesis. Mechanistically, loss of TECRL resulted in increased expression of GCN5, which enhances EGR2 transcription through acetylation. Ac-EGR2 binds to Pax7 promoter and enhances the expression of Pax7. These findings shed light on myogenic regeneration and muscle repair.

Materials and Methods

Detailed experimental methods including those for animal models, histology, isolation and FACS of satellite cells, cell cycle analysis, satellite cell colony assay, isolation and culture of single myofibers, RNAseq, satellite cell differentiation, construction of lentivirus overexpressing EGR2, construction of TECRL knockout lentivirus using CRISPR/Cas9, dual luciferase reporter assay, production and packaging of adeno-associated virus particles, AAV transduction in vivo, and statistical analysis can be found in *SI Appendix*.

Ethics Statement. All animal protocols were approved by the Institutional Laboratory Animal Care and Use Committee of Soochow University.

Data, Materials, and Software Availability. All relevant data are described within the manuscript and/or *SI Appendix*. The RNA-seq data have been deposited in the GEO database (GSE253890) (51).

ACKNOWLEDGMENTS. This work was supported by The National Natural Science Foundation of China (NSFC, No. 82370501 to Y.-H.S., 82370264 to Y.L., 81960072 to Y.S.), The Project of State Key Laboratory of Radiation Medicine and Protection, Soochow University (No. GZK12023023) to Y.L. The project for the Priority Academic Program Development of Jiangsu Higher Education Institutions (PAPD), Translational Research Grant of NCRCH (2020WSB07).

1. D. Akhmedov, R. Berdeaux, The effects of obesity on skeletal muscle regeneration. *Front. Physiol.* **4**, 371 (2013).
2. I. Dinulovic *et al.*, Muscle PGC-1alpha modulates satellite cell number and proliferation by remodeling the stem cell niche. *Skelet. Muscle* **6**, 39 (2016).
3. D. B. Gurevich *et al.*, Asymmetric division of clonal muscle stem cells coordinates muscle regeneration in vivo. *Science* **353**, aad9969 (2016).
4. A. L. Moyer, K. R. Wagner, Regeneration versus fibrosis in skeletal muscle. *Curr. Opin. Rheumatol.* **23**, 568–573 (2011).
5. A. Musaro, Muscle homeostasis and regeneration: From molecular mechanisms to therapeutic opportunities. *Cells* **9**, 2033 (2020).
6. H. C. Olguin, B. B. Olwin, Pax-7 up-regulation inhibits myogenesis and cell cycle progression in satellite cells: A potential mechanism for self-renewal. *Dev. Biol.* **275**, 375–388 (2004).
7. P. S. Zammit *et al.*, Muscle satellite cells adopt divergent fates: A mechanism for self-renewal? *J. Cell Biol.* **166**, 347–357 (2004).
8. M. A. Egerman *et al.*, GDF11 increases with age and inhibits skeletal muscle regeneration. *Cell Metab.* **22**, 164–174 (2015).
9. F. Relaix, D. Rocancourt, A. Mansouri, M. Buckingham, Divergent functions of murine Pax3 and Pax7 in limb muscle development. *Genes Dev.* **18**, 1088–1105 (2004).
10. F. Relaix, D. Rocancourt, A. Mansouri, M. Buckingham, A Pax3/Pax7-dependent population of skeletal muscle progenitor cells. *Nature* **435**, 948–953 (2005).
11. P. Seale *et al.*, Pax7 is required for the specification of myogenic satellite cells. *Cell* **102**, 777–786 (2000).
12. S. Kuang, S. B. Charge, P. Seale, M. Huh, M. A. Rudnicki, Distinct roles for Pax7 and Pax3 in adult regenerative myogenesis. *J. Cell Biol.* **172**, 103–113 (2006).
13. S. Oustanina, G. Hause, T. Braun, Pax7 directs postnatal renewal and propagation of myogenic satellite cells but not their specification. *EMBO J.* **23**, 3430–3439 (2004).
14. F. Relaix *et al.*, Pax3 and Pax7 have distinct and overlapping functions in adult muscle progenitor cells. *J. Cell Biol.* **172**, 91–102 (2006).
15. S. Gunther *et al.*, Myf5-positive satellite cells contribute to Pax7-dependent long-term maintenance of adult muscle stem cells. *Cell Stem Cell* **13**, 590–601 (2013).
16. C. Lepper, T. A. Partridge, C. M. Fan, An absolute requirement for Pax7-positive satellite cells in acute injury-induced skeletal muscle regeneration. *Development* **138**, 3639–3646 (2011).
17. M. M. Murphy, J. A. Lawson, S. J. Mathew, D. A. Hutcheson, G. Kardon, Satellite cells, connective tissue fibroblasts and their interactions are crucial for muscle regeneration. *Development* **138**, 3625–3637 (2011).
18. R. Sambasivan *et al.*, Pax7-expressing satellite cells are indispensable for adult skeletal muscle regeneration. *Development* **138**, 3647–3656 (2011).
19. J. von Maltzahn, A. E. Jones, R. J. Parks, M. A. Rudnicki, Pax7 is critical for the normal function of satellite cells in adult skeletal muscle. *Proc. Natl. Acad. Sci. U.S.A.* **110**, 16474–16479 (2013).
20. H. D. Devalla *et al.*, TECRL, a new life-threatening inherited arrhythmia gene associated with overlapping clinical features of both LQTS and CPVT. *EMBO Mol. Med.* **8**, 1390–1408 (2016).
21. P. Chavrier *et al.*, Structure, chromosome location, and expression of the mouse zinc finger gene Krox-20: Multiple gene products and coregulation with the proto-oncogene c-fos. *Mol. Cell Biol.* **9**, 787–797 (1989).
22. M. Mengozzi *et al.*, Erythropoietin-induced changes in brain gene expression reveal induction of synaptic plasticity genes in experimental stroke. *Proc. Natl. Acad. Sci. U.S.A.* **109**, 9617–9622 (2012).
23. D. Rubsamen *et al.*, IRES-dependent translation of egr2 is induced under inflammatory conditions. *RNA* **18**, 1910–1920 (2012).
24. Y. Gabet *et al.*, Krox20/EGR2 deficiency accelerates cell growth and differentiation in the monocytic lineage and decreases bone mass. *Blood* **116**, 3964–3971 (2010).
25. D. B. Parkinson *et al.*, Krox-20 inhibits Jun-NH2-terminal kinase/c-Jun to control Schwann cell proliferation and death. *J. Cell Biol.* **164**, 385–394 (2004).
26. P. Laslo *et al.*, Multilineage transcriptional priming and determination of alternate hematopoietic cell fates. *Cell* **126**, 755–766 (2006).
27. V. Lejard *et al.*, EGR1 and EGR2 involvement in vertebrate tendon differentiation. *J. Biol. Chem.* **286**, 5855–5867 (2011).
28. Z. Chen, J. I. Torrens, A. Anand, B. M. Spiegelman, J. M. Friedman, Krox20 stimulates adipogenesis via C/EBPbeta-dependent and -independent mechanisms. *Cell Metab.* **1**, 93–106 (2005).
29. F. A. Iannotti *et al.*, Genetic and pharmacological regulation of the endocannabinoid CB1 receptor in Duchenne muscular dystrophy. *Nat. Commun.* **9**, 3950 (2018).
30. G. C. Addicks *et al.*, MLL1 is required for PAX7 expression and satellite cell self-renewal in mice. *Nat. Commun.* **10**, 4256 (2019).
31. S. M. Hindi, A. Kumar, TRAF6 regulates satellite stem cell self-renewal and function during regenerative myogenesis. *J. Clin. Invest.* **126**, 151–168 (2016).
32. G. Zaman *et al.*, Loading-related regulation of transcription factor EGR2/Krox-20 in bone cells is ERK1/2 protein-mediated and prostaglandin, Wnt signaling pathway-, and insulin-like growth factor-I axis-dependent. *J. Biol. Chem.* **287**, 3946–3962 (2012).
33. Y. Wang *et al.*, The lysine acetyltransferase GCN5 is required for iNKT cell development through EGR2 acetylation. *Cell Rep.* **20**, 600–612 (2017).
34. G. C. Addicks *et al.*, GCN5 maintains muscle integrity by acetylating YY1 to promote dystrophin expression. *J. Cell Biol.* **221**, e202104022 (2022).
35. J. E. Turman Jr., N. B. Chopiuk, C. F. Shuler, The Krox-20 null mutation differentially affects the development of masticatory muscles. *Dev. Neurosci.* **23**, 113–121 (2001).
36. R. N. Niu, X. P. Shang, J. F. Teng, Overexpression of Egr2 and Egr4 protects rat brains against ischemic stroke by downregulating JNK signaling pathway. *Biochimie* **149**, 62–70 (2018).
37. Z. Gerhart-Hines *et al.*, Metabolic control of muscle mitochondrial function and fatty acid oxidation through SIRT1/PGC-1alpha. *EMBO J.* **26**, 1913–1923 (2007).
38. L. Wang *et al.*, GCN5 regulates FGF signaling and activates selective MYC target genes during early embryoid body differentiation. *Stem Cell Rep.* **10**, 287–299 (2018).
39. T. Uchida *et al.*, Reactive oxygen species upregulate expression of muscle atrophy-associated ubiquitin ligase Cbl-b in rat L6 skeletal muscle cells. *Am. J. Physiol. Cell Physiol.* **314**, C721–C731 (2018).
40. E. W. Bradley, M. M. Ruan, M. J. Oursler, Novel pro-survival functions of the Kruppel-like transcription factor Egr2 in promotion of macrophage colony-stimulating factor-mediated osteoclast survival downstream of the MEK/ERK pathway. *J. Biol. Chem.* **283**, 8055–8064 (2008).
41. M. Rozo, L. Li, C. M. Fan, Targeting beta1-integrin signaling enhances regeneration in aged and dystrophic muscle in mice. *Nat. Med.* **22**, 889–896 (2016).
42. X. Chen *et al.*, Akirin2 regulates proliferation and differentiation of porcine skeletal muscle satellite cells via ERK1/2 and NFATc1 signaling pathways. *Sci. Rep.* **7**, 45156 (2017).
43. Y. Hao *et al.*, Loss of CRY2 promotes regenerative myogenesis by enhancing PAX7 expression and satellite cell proliferation. *MedComm (2020)* 4, e202 (2023).
44. N. C. Jones, Y. V. Fedorov, R. S. Rosenthal, B. B. Olwin, ERK1/2 is required for myoblast proliferation but is dispensable for muscle gene expression and cell fusion. *J. Cell Physiol.* **186**, 104–115 (2001).
45. G. M. Smythe, J. K. Forwood, Altered mitogen-activated protein kinase signaling in dystrophic (mdx) muscle. *Muscle Nerve* **46**, 374–383 (2012).
46. A. E. Qualls, W. M. Southern, J. A. Call, Mitochondria-cytokine crosstalk following skeletal muscle injury and disuse: A mini-review. *Am. J. Physiol. Cell Physiol.* **320**, C681–C688 (2021).
47. C. S. Dela Cruz, M. J. Kang, Mitochondrial dysfunction and damage associated molecular patterns (DAMPs) in chronic inflammatory diseases. *Mitochondrion* **41**, 37–44 (2018).
48. D. V. Krysko *et al.*, Emerging role of damage-associated molecular patterns derived from mitochondria in inflammation. *Trends Immunol.* **32**, 157–164 (2011).
49. Q. Zhang *et al.*, Circulating mitochondrial DAMPs cause inflammatory responses to injury. *Nature* **464**, 104–107 (2010).
50. H. Dong, S. Y. Tsai, Mitochondrial properties in skeletal muscle Fiber. *Cells* **12**, 2183 (2023).
51. Y. Song *et al.*, Gastrocnemius muscle deletion of TECRL promotes skeletal muscle repair. NIBI Gene Expression Omnibus. https://www.ncbi.nlm.nih.gov/geo/query/acc.cgi?acc=GSE253890. Deposited 22 January 2024.